Stabilizing CO on Au with NO_2: Electronegative Species as Promoters on Coinage Metals?

Tianfu Zhang, Zhi-Pan Liu, S. M. Driver, S. J. Pratt, S. J. Jenkins, and D. A. King

Department of Chemistry, University of Cambridge, Lensfield Road, Cambridge, CB2 1EW, United Kingdom

(Received 16 August 2005; published 22 December 2005)

CO adsorption on NO_2-predosed Au{111} reveals an unexpected attractive coadsorbate interaction, associated with an unprecedented blueshift of the CO stretch frequency, a sizeable attenuation of the infrared NO_2 symmetric stretch band, and a $(\sqrt{7} \times \sqrt{7})R19°$ structure characterized by scanning tunneling microscopy and low energy electron diffraction. Density functional calculations allow us to rationalize these observations, and point towards a general pattern of behavior for electronegative coadsorbates on coinage metals, with important implications for catalytic promotion.

DOI: 10.1103/PhysRevLett.95.266102 PACS numbers: 68.43.Hn, 68.37.Ef, 68.43.Pq, 82.65.+r

The considerable activity of Au-based catalysts for various reactions has only recently emerged [1]. Although the low energy surfaces of metallic Au are catalytically inactive, the situation for dispersed nanoparticles on oxide supports is quite the reverse. Defects, metal/oxide interfaces, and electronic size effects have all been argued to influence activity [2,3], but the dominant factor may vary from one reaction to another. Further enhancement of the catalytic activity might be effected by adding reactive transition elements, and our own recent efforts have considered the effect of Ir in enabling NO_x reduction over Au. During our initial characterization of NO_x adsorption on clean Au{111}, however, we were astonished to discover the dramatic influence of NO_2 in activating this inert substrate for CO adsorption [4], giving rise to an unexpected enhancement of the CO adsorption energy and a remarkable blueshift of the CO stretch frequency. Since stronger adsorbate-substrate binding on metals typically correlates with a *red*shift of the CO stretch, these last two effects would seem to be contradictory and warranted further exploration. Combining vibrational spectroscopy with scanning tunneling microscopy (STM) and first-principles density functional theory (DFT) calculations, we have been able to reconcile the contradictions within a fully unified description of this coadsorption system. We reveal the unanticipated *attractive* interaction between CO and electronegative species to be a general phenomenon on Au surfaces, which may have profound implications for the development of catalytic technologies using coinage metals.

In order to elucidate the nature of the above phenomenon, we prepared mixed adlayers on Au{111} under controlled conditions at 115–140 K by preadsorbing NO_2 and then deliberately dosing CO. Reflection-absorption infrared spectroscopy (RAIRS), temperature-programmed desorption (TPD), low energy electron diffraction (LEED), and STM experiments were carried out in two ultrahigh vacuum chambers, described elsewhere [5]. Our results show that although CO does not adsorb on clean Au{111} at $\sim$120 K and 5×10^{-8} mbar, the molecule readily adsorbs at this temperature in the presence of preadsorbed NO_2.

Following cycles of Ar ion sputtering and a short anneal at 800 K for 120 s, the clean Au{111} surface exhibited the characteristic satellite LEED pattern associated with the $(\sqrt{3} \times 22)$ rect. "herringbone" reconstruction and an Auger spectrum free of contaminants. On adsorption of NO_2 alone at 135 K, the satellite spots attenuate with increasing exposure until a sharp (1×1) pattern from the unreconstructed substrate is observed. Other authors have calibrated the coverage and report complete lifting of the reconstruction with 0.15 ML NO_2 [6]; we assert that this occurs without formation of an ordered NO_2 overlayer at such low coverage and temperatures in the range 100–135 K [7]. The subsequent adsorption of CO gives rise to a new LEED pattern, comprising two mirror domains of $(\sqrt{7} \times \sqrt{7})R19°$ periodicity, which disappears after a few seconds due to electron-stimulated processes.

The RAIR spectrum of an NO_2 layer at 115 K (Fig. 1) shows a single band at 1179 cm^{-1} that is readily assigned to the symmetric stretch of a nitrito species, bonded to the substrate through its oxygen atoms [6,9]. Because of practical constraints, it was impossible to correlate coverages between our LEED and RAIRS experiments; we are therefore unable to quantify the NO_2 coverage of our RAIRS experiments, but note that similar spectra were obtained across a finite (unknown) coverage range. When the NO_2-predosed surface is exposed to CO, two new infrared bands appear in the spectrum at 2186 and 2174 cm^{-1} (Fig. 1) and the NO_2 band remains with reduced intensity.

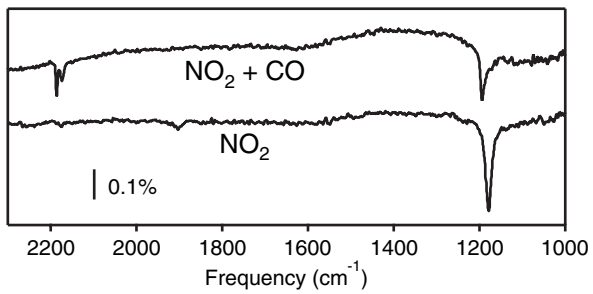

FIG. 1. RAIR spectra at 115 K of NO_2 on Au{111} (lower trace) and after subsequent saturation with CO (upper trace).

Repeating the experiment with $^{13}C^{18}O$ yields isotopic frequency shifts that confirm both bands to be C-O stretches and suggest that they derive from a coadsorption structure of NO_2 with CO, rather than a surface reaction product. On heating, two CO desorption peaks are detected in TPD at 145 and 160 K, correlating with disappearance of the two CO infrared bands. We consistently observed the 2186 cm^{-1} peak to disappear more readily when the temperature is held in the range 115–130 K; we therefore conclude that the higher (lower) frequency CO stretch correlates with the TPD peak at 145 K (160 K). As CO desorbs, the NO_2 band intensity is restored to its original value, indicating that the observed CO-induced intensity drop is due to either a structural or an electronic change, rather than displacive desorption of NO_2.

STM images were obtained in constant current mode at 77 or 5 K. Following CO adsorption with near-saturation NO_2 precoverage, large area scans taken at many points on the surface show it to be almost completely covered by domains of $(\sqrt{7} \times \sqrt{7})R19°$ periodicity with a honeycomb arrangement of bright protrusions (Fig. 2). Subsidiary protrusions can be seen in the center of each honeycomb ring, while deep holes occasionally occur where a bright protrusion is missing. By comparison with images of a pure adlayer, we tentatively attribute the brightest asperities to NO_2, the dimmer features to CO, and the holes to NO_2 vacancies. This interpretation implies local NO_2 and CO coverages of 3/7 and 1/7 ML, respectively. Further experiments with lower NO_2 precoverage show islands of the same $(\sqrt{7} \times \sqrt{7})$ structure, together with less highly ordered regions of lower local NO_2:CO ratio and patches of bare substrate [8]. We conclude that the $(\sqrt{7} \times \sqrt{7})$ LEED pattern derives solely from the coadsorption structure imaged in Fig. 2.

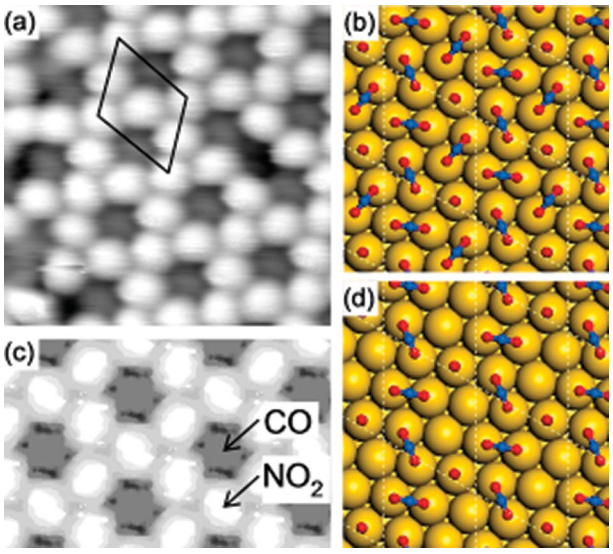

FIG. 2 (color). (a) STM image (28×28 Å^2, gray scale range 1.5 Å, sample bias +0.10 V, current 1.0 nA) of an NO_2 + CO coadsorbed layer, corresponding to the 3:1 structure shown in (b); (c) corresponding DFT Tersoff-Hamann simulation [16]; (d) 2:1 model, for comparison.

Our experiments highlight two remarkable findings: first, an attractive interaction between CO and an electronegative coadsorbate; second, a blueshift of the coadsorbed CO stretch frequency with respect to the gas phase value, a phenomenon only previously reported on cationic metal sites. Both effects are unexpected and neither is small. The attractive interaction induces CO adsorption on Au{111} at 120 K under vacuum conditions, while the blueshift of up to 43 cm^{-1} falls in the range of those observed on metal oxides. Any model purporting to explain these phenomena must also be consistent with the potentially revealing drop in NO_2 band intensity upon coadsorption. We emphasize, however, that energetic and vibrational characteristics are inevitably intertwined, and that both can be addressed via electronic structure calculations within the DFT framework, performed here using the CASTEP code [10,11].

We began by eliminating many possible association reaction products, including the sole example consistent with only a *symmetric* NO_2 stretch in the RAIR spectrum (i.e., upright $OCNO_2$). Our calculations confirmed these species to be unstable, in line with our interpretation of the observed isotopic shifts. In all further DFT work we explored coadsorption of NO_2 and CO with the experimentally observed $(\sqrt{7} \times \sqrt{7})$ periodicity, considering several possible coverages and structures. Of the models investigated, the most stable structures exhibit a number of common features. In particular, NO_2 preferentially adopts an upright nitrito configuration, bridging between two adjacent Au atoms and consistent with the infrared spectra described above. Furthermore, CO adsorbs in an atop site next to NO_2, but configurations where the three Au atoms involved in binding the molecules form an equilateral triangle are energetically unfavorable.

Our further discussion focuses on the three models that are most stable for 1/7 ML CO coadsorbed with 1/7, 2/7, and 3/7 ML NO_2 (hereafter termed the 1:1, 2:1, and 3:1 models; Figs. 2 and 3). The adsorption energy of CO on clean Au{111} is calculated as just 0.18 eV, whereas in the presence of NO_2 it rises to approximately 0.33 eV; this increase, however, is only weakly dependent upon the NO_2

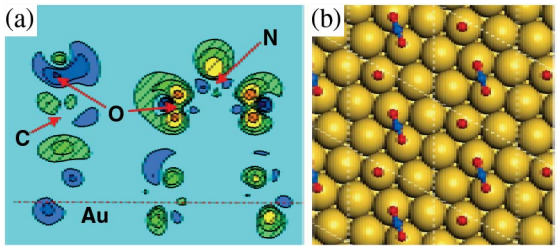

FIG. 3 (color). (a) Charge redistribution occurring when isolated adsorbed CO and NO_2 are superposed to form the mixed 1:1 phase (b). Red/yellow/green (dark blue) regions show electron density increase (decrease).

coverage (Table I). These enhanced adsorption energies are entirely consistent with our TPD data, where CO desorption from the coadsorbed phase peaks at 145–160 K.

Calculated CO frequencies for the three model structures are all markedly blueshifted with respect to the value on clean Au{111}, ranging between 2172–2206 cm^{-1} (Table I). The shift relative to the clean surface is almost linear in the number of NO_2 molecules per unit cell. The precise values for the 1:1 and 2:1 structures are closest to the bands observed in experiment, but we acknowledge both their small separation and the intrinsic uncertainty in determining absolute vibrational frequencies from DFT. It is likely that the two observed CO bands actually correspond to the 3:1 structure and the less highly ordered phase seen in STM. We tentatively suggest that the sharp higher frequency CO stretch corresponds to the former and the broader low frequency peak to the latter.

Our calculations also provide insight into the CO-induced attenuation of the NO_2 infrared absorption. As reorientation of NO_2 is precluded, since the molecule retains an upright geometry in all of the most stable coadsorption structures, we consider the influence of CO on the NO_2 dynamic dipole moment. This we have calculated by monitoring changes in work function upon finite displacements of the NO_2 molecule according to the appropriate vibrational eigenfunction [13]. We calculate that CO coadsorption causes a 20% decrease of the NO_2 band intensity (proportional to the square of dynamic dipole moment) at 2/7 and 3/7 ML NO_2, but has no influence at 1/7 ML. This behavior is broadly consistent with the observed intensity change (ranging from 25–50 ± 5%).

Having demonstrated the ability of DFT to describe the main features of our coadsorption experiments, we can now confidently interrogate the simulated charge density to elucidate the nature of the attractive interaction. We begin by examining each adsorbate in isolation on the surface. Both CO and NO_2 accumulate negative charge on adsorption, constituting electric monopoles of charge -0.02 and $-0.45e$ respectively. They differ, however, in their dipolar character. In the case of CO, the adsorbate dipole is directed parallel to the surface dipole, while for NO_2 it is antiparallel. There is therefore an attractive dipolar contribution to the adsorption energy of NO_2, but a repulsive contribution for CO. The latter is nevertheless marginally surpassed by the molecule's orbital interactions with the surface.

TABLE I. DFT results for 1/7 ML CO adsorption on Au{111}/X (X = NO_2, S, O, Cl; coverage θ_x). E_{CO}, ν_{CO}, and d_{CO} are the adsorption energy, corrected stretch frequency, and bond length of CO [11].

	θ_x/ML	E_{CO}/eV	ν_{CO}/cm^{-1}	d_{CO}/Å
Au	0	0.18	2151	1.15
Au/NO_2	3/7	0.35	2206	1.14
Au/NO_2	2/7	0.33	2189	1.14
Au/NO_2	1/7	0.32	2172	1.15
Au/S	1/7	0.24	2140	1.15
Au/O	1/7	0.31	2156	1.15
Au/Cl	1/7	0.30	2141	1.15

As on all metals, the chemical bonding of CO with Au may be described in terms of electron donation from the molecular 5σ; orbital to the metal, together with back-donation from the metal to the $2\pi^*$ orbital [14]. The predominant interaction of NO_2 with the surface involves the $6a_1$ molecular orbital, which is half filled in the gas phase and further filled upon adsorption. These charge redistributions should be understood as resulting from the covalent mixing of adsorbate and substrate orbitals, rather than as ionic processes. Unlike other transition elements, however, all the coinage metals (Cu, Ag, Au) have a filled valence d band lying some way below the Fermi level; the substrate states contributing to chemisorption therefore derive mainly from the s/p band. The resulting mixed states consequently appear quite localized on the molecule, but with a considerable delocalized component permeating the metal selvedge.

In order to investigate the mutual interaction between the coadsorbates, we present the electron density difference, representing the change that occurs when well-separated adsorbates are brought together to form a mixed 1:1 structure (Fig. 3). The most important features are depletion of electron density from the CO $2\pi^*$ mixed state and accretion of electron density in both the CO 5σ and NO_2 $6a_1$ mixed states relative to the isolated adsorbates. These effects weaken the adsorbate-substrate covalent bonding of CO, while strengthening that of NO_2, but also influence the molecular monopoles: the NO_2 monopole becomes more negative ($-0.48e$) while CO becomes slightly positive ($+0.04e$). Furthermore, the redistribution of charge enhances the NO_2 dipole, and reduces that of adsorbed CO. Thus the mutual interaction between the coadsorbates comprises covalent, monopolar, and dipolar contributions, all of which may be significant in the present case.

Considering that the isolated adsorbates are both negatively charged, we might have expected their mutual monopolar interaction to be repulsive; in fact, the charge redistribution just described implies a weak attraction in the coadsorbed geometry. In contrast, the expected attractive interaction between the antiparallel dipoles of the isolated adsorbates is probably somewhat reduced by the NO_2-induced depolarization of CO. Although these effects are not easy to quantify, it is reasonable to assume that they offset each other to a certain degree. Similarly, the reduced adsorbate-substrate covalent bonding of CO is presumably counterbalanced, to some extent, by strengthening that of NO_2; it is not obvious therefore whether the net change in covalent bonding is positive, negative, or nearly zero. Finally, we must consider the interactions of the adsorbate dipoles with the surface dipole. In the coadsorbed geometry, the reduced CO dipole provides a less repulsive interaction with the surface than for the isolated adsorbate,

while the enhanced NO_2 dipole leads to a greater attractive interaction with the surface. Both effects necessarily contribute favorably to the net attractive interaction between CO and NO_2 upon coadsorption.

Although there is no single cause of this net coadsorbate attraction, the foregoing discussion does, however, allow us to resolve the individual contributions. The largest coadsorbate repulsion probably arises from decreased covalent bonding between CO and the surface, while the largest coadsorbate attraction seems likely to arise from the complementary increased covalent bonding between NO_2 and the substrate, albeit supplemented by potentially crucial changes in the electrostatic interactions between molecular and surface dipoles. We emphasize that the issue of whether the overall coadsorbate interaction is attractive or repulsive emerges from the detailed balance of all the terms discussed above, and that to focus only upon the largest individual terms would be overly simplistic.

The insight provided by DFT also yields some explanation for the CO blueshift observed in experiment. Depleting the $2\pi^*$ mixed state, relative to the isolated adsorbate, ought to cause a blueshift that outweighs the redshift caused by repopulation of the 5σ (the former is more antibonding than the latter). Furthermore, the presence of the adjacent antiparallel molecular dipole of coadsorbed NO_2 provides an additional electrostatic restoring force that will also contribute to the observed blueshift. These two effects result in a CO stretch frequency substantially higher than the gas phase value.

Our results demonstrate that the interaction between two electronegative adsorbates need not necessarily be repulsive, and lead us to question whether this observation might extend to other CO coadsorption systems. We have therefore performed DFT calculations for $(\sqrt{7} \times \sqrt{7})$ 1:1 structures with O, S, and Cl in *fcc* hollow sites replacing bridging NO_2. The results indicate attractive interactions of comparable magnitude to that found for NO_2 (Table I). In contrast, however, the CO stretch frequency remains close to its calculated value for clean Au{111}. The charge density difference plots for these atomic coadsorbates are broadly similar to that shown in Fig. 3, but with somewhat less depletion of the CO $2\pi^*$ mixed state, and no large antiparallel dipole associated with the adatom. We are aware of just one relevant example in the literature, where CO is stabilized to 90 K on Ag{111} by coadsorbed Cl [15]. We note that our present calculations do not support the explanation proposed in that work; we find no evidence of significant Cl-induced changes in the *d* band of Au{111}, nor of Cl-induced depopulation of the 5σ state.

Contrary to expectations, we have identified four exemplary systems in which electronegative coadsorbates stabilize CO on Au{111}. Unlike the case of electropositive coadsorbates, however, the stabilization is not associated with any significant decrease in the strength of the C-O bond. In consequence, an electronegative coadsorbate may promote CO adsorption on coinage metals, but will not directly reduce the barrier to CO dissociation. The ability to bind CO more strongly, however, may nevertheless be indirectly beneficial in allowing dissociation to become competitive with desorption. Even so, the effect of electronegative coadsorbates in enhancing CO adsorption may, perhaps, best be harnessed in promoting association reactions on coinage metals. The typecasting of electronegative species as catalytic poisons does not therefore seem entirely justified; our results indicate that on coinage metals they can play precisely the opposite role. We hope that this conclusion will stimulate further work to verify the promotion of specific catalytic reactions and to establish the magnitude of any such effect.

We thank the Newton Trust, Toyota, EPSRC and The Royal Society for funding, and Dr. D. Escott for technical assistance.

[1] M. Haruta, Catal Today **36**, 153 (1997).
[2] Z.-P. Liu, S. J. Jenkins, and D. A. King, Phys. Rev. Lett. **93**, 156102 (2004); **94**, 196102 (2005).
[3] M. Valden, X. Lai, and D. W. Goodman, Science **281**, 1647 (1998); M. Schubert *et al.*, J. Catal. **197**, 113 (2001); Z.-P. Liu P. Hu, and A. Alavi, J. Am. Chem. Soc. **124**, 14 770 (2002).
[4] Although we did not, at first, intentionally dose CO, it is one of the residual gases within the uhv chamber.
[5] R. Raval *et al.*, J. Vac. Sci. Technol. A **9**, 345 (1991); C. I. Carlisle *et al.*, Surf. Sci. **470**, 15 (2000).
[6] M. E. Bartram and B. E. Koel, Surf. Sci. **213**, 137 (1989).
[7] Our STM experiments revealed NO_2 islands of $c(2 \times 4)$ structure with 0.25 ML local coverage at 78 K [8]. A $(\sqrt{3} \times \sqrt{3})R30°$ LEED pattern is reported at 100 K and approximately 0.25 ML NO_2 [6].
[8] T. Zhang, S. M. Driver, and D. A. King (to be published).
[9] J. Wang and B. E. Koel, J. Phys. Chem. A **102**, 8573 (1998).
[10] M. C. Payne *et al.*, Rev. Mod. Phys. **64**, 1045 (1992).
[11] Wave functions were expanded in a plane wave basis to a 340 eV cutoff, with a $4 \times 4 \times 1$ *k*-point mesh. Ultrasoft pseudopotentials and PBE [12] exchange-correlation functional were employed. The surface was modeled by a four-layer slab with two relaxed layers. Vibrations were calculated by finite displacements. A positive offset of 90 cm^{-1} was applied to all adsorbed CO frequencies based on comparison with a known DFT underestimate for CO/Au{110}.
[12] J. P. Perdew, K. Burke, and M. Ernzerhof, Phys. Rev. Lett. **77**, 3865 (1996).
[13] P. J. Feibelman, Phys. Rev. B **67**, 035420 (2003).
[14] G. Blyholder, J. Phys. Chem. **68**, 2772 (1964); P. Hu *et al.*, Chem. Phys. Lett. **246**, 73 (1995).
[15] K. Kershen *et al.*, Langmuir **17**, 323 (2001).
[16] J. Tersoff and D. R. Hamann, Phys. Rev. B **31**, 805 (1985).